AD

TECHNICAL REPORT ARCCB-TR-03016

FACTORS AFFECTING CHROME LOSS IN GUN TUBES

Paul J. Cote, Mark E. Todaro, Mark Witherell

DECEMBER 2003

US ARMY ARMAMENT RESEARCH,
DEVELOPMENT AND ENGINEERING CENTER
Close Combat Armaments Center
Benét Laboratories
Watervliet, NY 12189-4000

TACOM-ARDEC

APPROVED FOR PUBLIC RELEASE; DISTRIBUTION UNLIMITED

REPORT DOCUMENTATION PAGE

Form Approved
OMB No. 0704-0188

1. AGENCY USE ONLY (*Leave Blank)*	2. REPORT DATE	3. REPORT TYPE AND DATES COVERED
	NOVEMBER 2003	FINAL

4. TITLE AND SUBTITLE

Factors Affecting Chrome Loss in Gun Tubes

5. FUNDING NUMBERS
AMCMS No.
4221 230 0000

6. AUTHORS

Paul J. Cote, Mark E. Todaro, Mark Witherell

7. PERFORMING ORGANIZATION NAME(S) AND ADDRESS(ES)

US Army ARDEC
Benét Laboratories, AMSTA-AR-CCB-O
Watervliet Arsenal, NY 12189-4000

8. PERFORMING ORGANIZATION REPORT NUMBER
ARCCB-TR-03016

9. SPONSORING / MONITORING AGENCY NAME(S) AND ADDRESS(ES)

US Army ARDEC
Close Combat Armaments Center
Picatinny Arsenal, NJ 07806-5000

10. SPONSORING / MONITORING AGENCY REPORT NUMBER

11. SUPPLEMENTARY NOTES

12a. DISTRIBUTION / AVAILABILITY STATEMENT

Approved for public release; distribution unlimited.

12b. DISTRIBUTION CODE

13. ABSTRACT *(Maximum 200 words)*

The objective of the study was to gain further insights into the origin of chromium loss in tank guns. The present report summarizes the results of a study surveying chromium loss at various critical locations along a 120-mm M256 tank gun tube. Tube no. 6824 was selected because it had fired relatively few rounds (119), while still exhibiting initiation of all the typical chromium damage features in the chamber and bore of a 120-mm tube. Coating stresses were also computed with a finite element model to aid in the analyses. The data reveal a broad range of metallurgical effects related to erosion damage at the bore surface during firing. Establishing the cause of chromium loss in any specific case can be difficult because of the numerous contributing factors. Nevertheless, the present data show that high temperature oxidation at the chromium/steel interface is a common feature in both the chamber and the gun bore, indicating that steel oxidation is an essential factor in chromium loss. The interface oxidation occurs by gas penetration through chromium cracks that extend from the coating surface to the interface. This oxidation undermines the chromium coating and promotes chromium spallation, which then leads to pitting in the chamber and erosion in the bore.

14. SUBJECT TERMS

Chromium, spallation, 120-mm tank gun, finite element modeling, chamber pitting

15. NUMBER OF PAGES
28

16. PRICE CODE

17. SECURITY CLASSIFICATION OF REPORT	18. SECURITY CLASSIFICATION OF THIS PAGE	19. SECURITY CLASSIFICATION OF ABSTRACT	20. LIMITATION OF ABSTRACT
UNCLASSIFIED	UNCLASSIFIED	UNCLASSIFIED	UL

TABLE OF CONTENTS

LIST OF TABLES AND FIGURES

INTRODUCTION

A detailed study of chromium loss along the chamber and bore of a typical 120-mm tank gun tube was performed to provide insights into the general problem of chromium loss in tank guns. Tank guns are coated with electro-deposited chromium to protect the bore surface against erosion from high energy propellants.

The chamber houses the propellant that is contained within a combustible cartridge case. The chamber generally experiences lower temperatures than the bore as a consequence of the lower gas velocities in the chamber relative to the bore. Because the chamber walls are thinner than bore walls, chromium loss and subsequent corrosion pitting at this location tends to produce early fatigue cracks. By contrast, chromium loss in the thick-walled bore often reduces service life because of loss of accuracy attributable to rapid metal loss by melting/erosion of the exposed steel.

Pitting in the chamber and erosion in the bore are competing issues in limiting the service life of a tank gun. Our aim was to establish the major chromium loss factors by analyzing damage along the length of a tube that exhibited all the typical chromium damage features. A tube with a relatively small number of fired rounds was selected so that extensive erosion damage did not mask the damage initiation process. Another aim of the study was to establish the possible causes of severe pits in the chamber.

The 120-mm M256 tube no. 6824 fit the criteria for a representative tube. It had fired a total of 119 rounds where the last 40 were high energy (A3) rounds. The chamber and bore exhibited typical chromium damage seen in most tubes: generally, the back half of the chamber is relatively free of chromium damage, while the forward half of the chamber exhibits progressively increasing chromium loss and pitting initiation along the tube axis towards the bore. The bore exhibited the usual melt erosion seen with high energy propellants. In both the chamber and bore, initial chromium loss is manifested by chromium islands that have detached from the steel and are raised above the chromium surface. These raised islands usually become polished and often appear as bright spots to the unaided eye. These islands eventually are completely removed, leaving a random distribution of holes in the chromium.

The chromium crack pattern that leads to the island configuration originally forms from extensive cracking during the electro-deposition of the high contractile chromium. The chromium surface cracks widen on subsequent heat treatment at about 200ºC to outgas hydrogen and widen further on firing. With high contractile chromium, the chromium islands also exhibit a high density of fine embedded cracks distributed randomly throughout their volumes. Embedded cracks are formed by repeated cracking and overplating during the chromium electro-deposition process.

Representative specimens were obtained at selected locations all along the chamber and bore to allow us to metallographically evaluate the various damage mechanisms. Much of the discussion of damage mechanisms is based on results of our earlier general studies of the initiation of bore coating damage (1,2).

EXPERIMENTAL METHODS

Specimens were prepared from areas of interest along the axis of the chamber and bore of M256 gun tube no. 6824 to permit evaluation of details of the damage to the chromium and steel in the vicinity of the interface at the various locations. As mentioned earlier, gun tube no. 6824 fired a total of 119 rounds where the last 40 were the high temperature A3 rounds. Subsequent to firing the 119 rounds, tube no. 6824 was fatigue tested at Benet using the hydraulic fatigue test facility prior to the present study. Numerous fine fatigue cracks from 8264 cycles in the hydraulic test are present in the specimen. These cracks are easily distinguished from corroded and debris-filled cracks that form during firing. The data in the present study were taken from regions that do not contain cracks from the fatigue test. Optical microscopy, confocal microscopy, electron microprobe analysis, SEM, and EDAX were used for the analyses.

RESULTS

Figure 1 is a schematic showing the approximate location of the specimens prepared for this study. Position no. 1 (~10 in. from the rear face of the tube [RFT]) exhibits no chromium loss. Position

no. 1 is just forward of the breech ring, as indicated in the figure. Position no. 2 is taken from the central region of chrome loss (chromium island lifting) and pitting initiation (~14 in. from RFT). Position no. 3 represents the bore origin (~20 in. from RFT) and shows no chromium loss. Position no. 4 is a downbore location (~35 in. from RFT) and shows chromium loss (chromium island lifting) and pitting initiation.

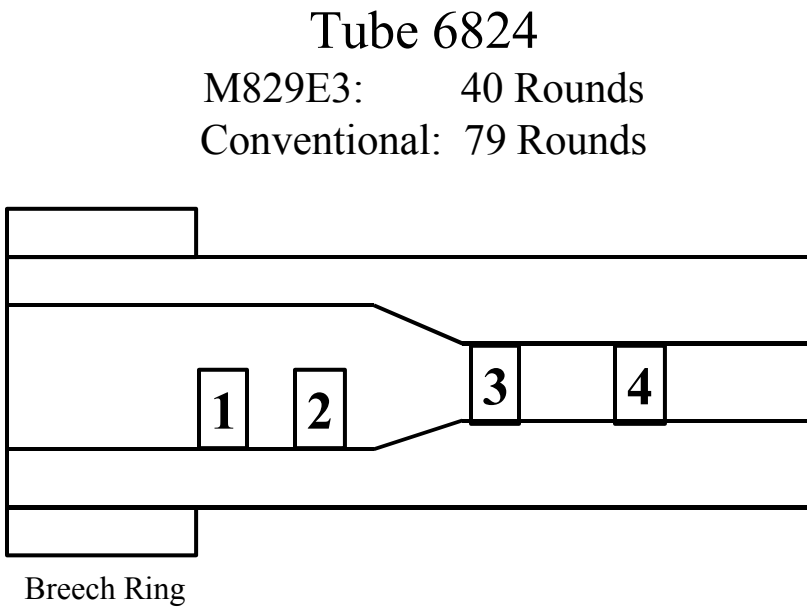

Figure 1. Schematic of 120-mm tank gun section (tube 6824) showing four locations where chromium damage was assessed in the present study.

Figure 2 shows top views of the chromium coating at the four positions. Circumferential surface grinding marks are present on the chromium surface. They appear as fine grooves that run perpendicular to the tube axis. The chromium surface in the chamber is often ground to bring dimensions to specification. There are no grinding marks at the downbore position (no. 4), as the grinding operation does not extend downbore. Examples of chrome island lifting are shown at positions no. 2 and 4. Examination of many such examples has shown us that the island loss at these positions is progressive, starting with lifting of a corner and continuing in stages until the entire island lifts away from the steel substrate. The interaction of the combustible case with the ground chrome surface provides fortuitous evidence of the nature of the damage experienced by the chromium because the sliding of the case

against the chromium serves to provide a fine polish on raised portions of the chromium. Some evidence of this polishing can be seen in the micrograph at position no. 2. Note that the polishing is preferential along the chromium island edges that are aligned in the axial direction. Also, the widths of the chromium cracks that are aligned along the axial direction are generally significantly larger than those at other orientations. By contrast, the micrograph at position no. 4, in the bore, shows a significantly larger increase in crack widths, and this increase occurs uniformly for all orientations along the chromium surface.

Surface of M256 Tube #6824. (1,2 Chamber; 3,4 Bore)
Mean Chromium hardness; arrows indicate tube axis

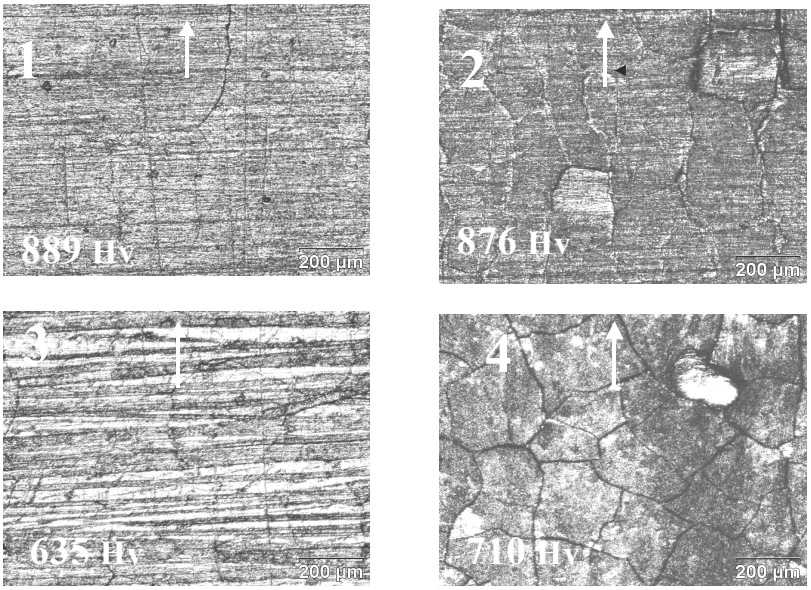

Figure 2. Micrograph of top surface of specimens from the four locations indicated in Figure 1. Examples of island lifting are shown for locations 2 and 4. (Surface of M256 tube 6824; mean chromium hardness; arrows indicate tube axis [1 and 2 are from the chamber; 3 and 4 are from the bore].)

The chromium surface at position no. 3 shows significant deformation along bands that have a roughly circumferential orientation. Evidently, fragments of the combustible case or material within the propellant packaging become wedged under the obturator during firing to produce the observed indentations. This is another indication of high temperature softening in the chromium.

Mean chromium hardness through the thickness of the tube is shown in Table 1 and in the figure. The chromium in the chamber essentially maintains its original hardness near 900 kg/mm^2. The maximum chromium softening from the heating effects of firing occurs at the bore origin (position no. 3).

Table 1. Mean Chromium Hardness

Position	no. 1	no. 2	no. 3	no. 4
Vickers Hardness (kg/mm^2)	889	876	635	710

Figure 3 shows micrographs of a section from position no. 1. There is no chromium loss and only a few indications of oxidation initiation at the tips of the widest chromium crack. As illustrated in Figure 1, the position no. 1 location is just forward of the breech ring. One generally sees little indication of chromium loss in the first half of the chamber, which is under the breech ring. There is some preferential edge polishing indicating some deformation, but it is not as pronounced as that seen at position no. 2 in the second half of the chamber (adjacent to the bore origin).

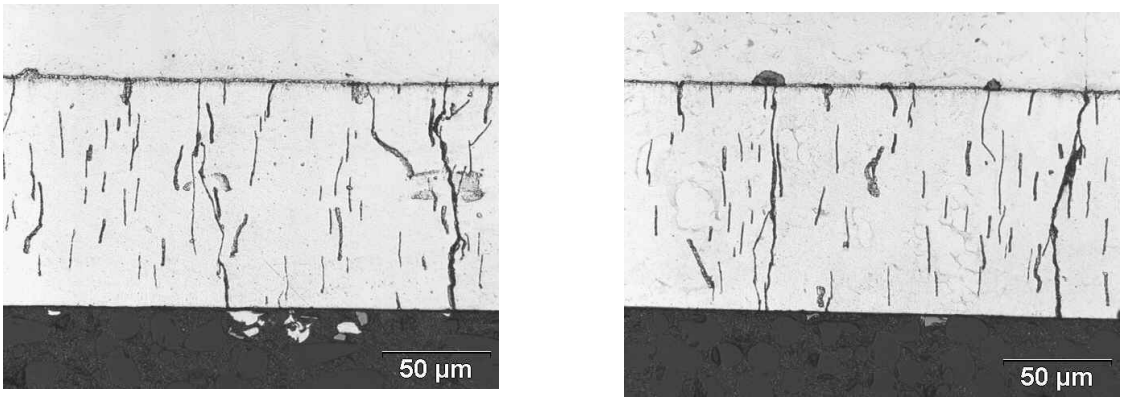

Figure 3. Micrograph of section of a specimen from position no. 1 (midchamber) showing relatively little damage. Through cracks, embedded cracks, and the initiation of some corrosion at the chromium crack tips is observed.

Figure 4 shows micrographs of a section from position no. 2 in the chamber area adjacent to the bore origin where chromium island lifting and pitting initiation is observed. There is substantial

evidence of oxidation at many sites along the interface. The embedded cracks have grown and linked to allow penetration of propellant gas to the vulnerable steel at the interface, as is evident from the numerous sites of hot corrosion along the interface within each individual chromium island. Chromium is lost by complete separation of the island from the substrate. There are also numerous examples of unusual loss of chromium sections by fracture of the chromium islands parallel to the interface, as shown in the figure. There is no indication of significant extension of the chromium cracks into the steel substrate anywhere in the chamber as a result of the 119 fired rounds.

Chromium/steel at position #2

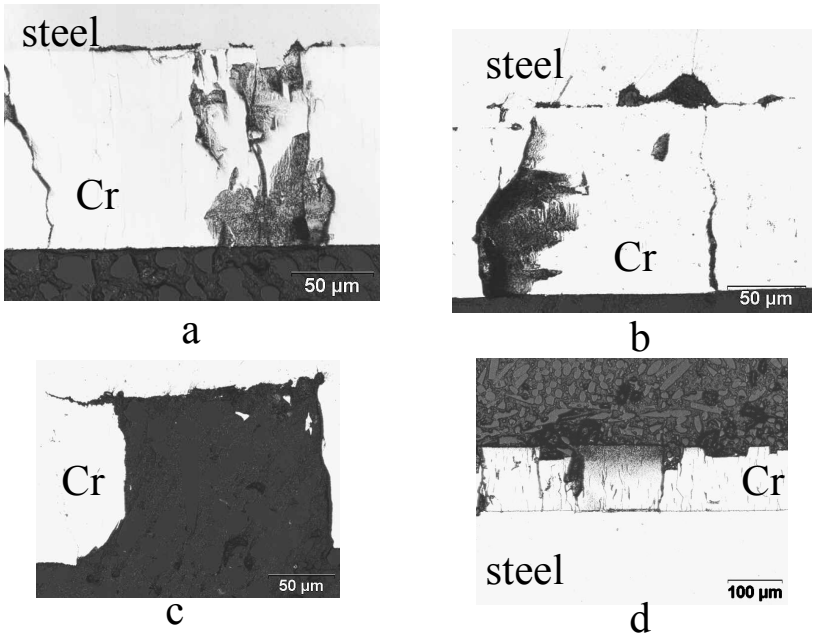

Figure 4. Micrograph of section of a specimen from position no. 2 (chamber region close to bore origin) showing considerable chromium fracture, spallation, and interface corrosion.

Figure 5 offers an enlarged image of the polishing effect on the raised edges of the chromium islands at position no. 2 in the chamber. (see, also, Figure 2, no. 2). The arrow indicates tube axis orientation, which is perpendicular to the grinding marks on the chromium. The raised portions of the chromium are preferentially aligned axially, as are the widened chromium cracks. They are consistent with damage caused by cyclic mechanical chamber expansion and contraction in the hoop direction from pressurization. (Thermal effects are biaxial in the plane of the surface, and, thus, are not expected to

show orientation effects. See Figure 2, no. 4.) Height mapping using confocal microscopy confirmed that the polished edges of the chromium islands are raised above adjacent surfaces.

Position #2 surface showing preferential edge lifting

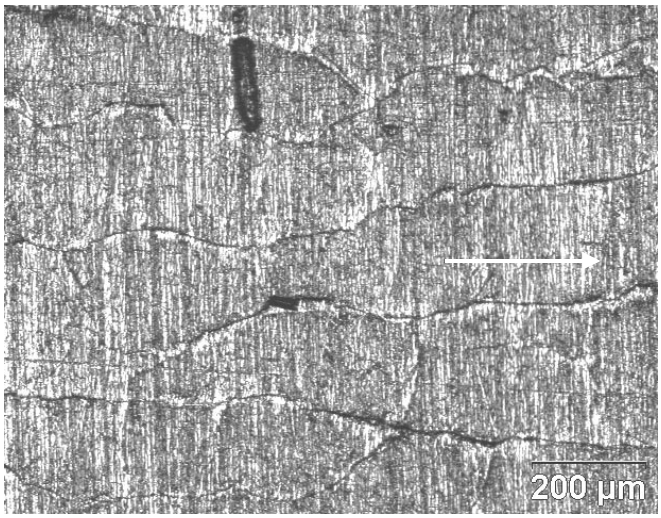

Figure 5. Micrograph showing top view of chromium at chamber position no. 2 showing pronounced edge lifting indicated by polishing effect at crack edges that are aligned axially.

Figure 6 shows micrographs at position no. 3, corresponding to the origin of the bore at the approximate location of the obturator. There is no evidence of chromium loss or pitting initiation at this position, despite there being a general extension of the chromium cracks into the steel, as well as significant hot corrosion at the interface (at the chromium crack tips), a heat-affected zone in the steel, and observable chromium diffusion into the steel ("chromizing"). The chromium has clearly recrystallized and reached the grain growth stage at the outer portions of the coating (white colored grains). The plastic deformation bands on the top of the chromium seen earlier in Figure 2 are reflected in the flow lines evident at the top of the chromium in the large grain portion of the chromium.

Although substrate cracking at the chromium crack tips from the 119 fired rounds is most pronounced at this location, with several cracks extending to roughly 30 µmas seen in Figure 6c, such

cracking is, nevertheless, relatively sparse. Metal consumption from high temperature oxidation appears to be the dominant damage mechanism.

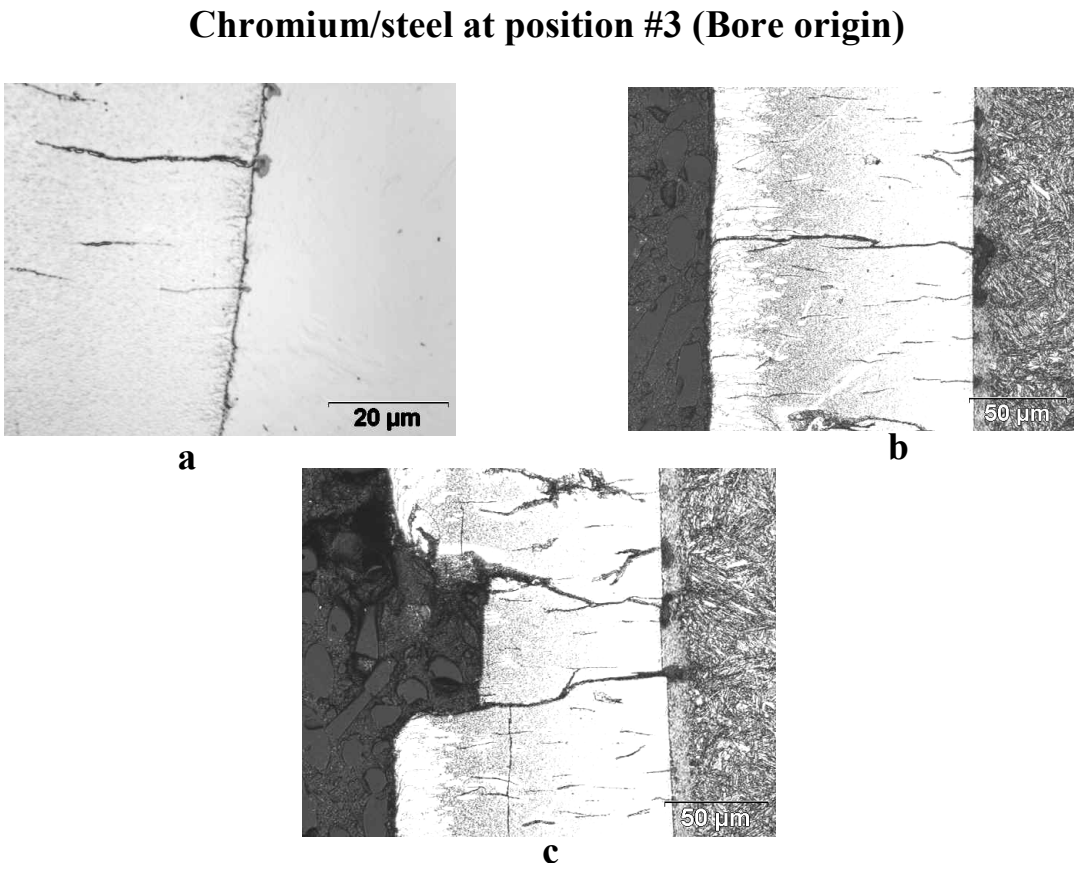

Figure 6. Micrograph showing sections through specimen at position no. 3 (bore origin). This location has experienced the highest temperatures as indicated by the chromium transformations and heat affected zone in the steel. Figure 6a is unetched to show corrosion, and Figures 6b and 6c were etched to reveal the heat affected zones. Although the steel at this location is not heavily cracked, the deepest substrate cracks occur at this location as shown in 6band 6c. There is no chromium island loss.

Figure 7 shows micrographs at position no. 4, corresponding to approximately 13 in. downbore where chrome island loss occurs and some pitting is observed. Unlike position no. 3 (bore origin), the downbore location exhibits no heat-affected zone, no observable chromium diffusion into the steel, and no significant grain growth in the chromium. Although not evident in this figure, there is a relatively thick layer of firing debris (~3-5 µm) covering the top of the chromium and extending into all the

chromium cracks. As indicated in the top view (Figure 2, no. 4) the cracks are generally wider here (~6 μm) than at any of the other locations.

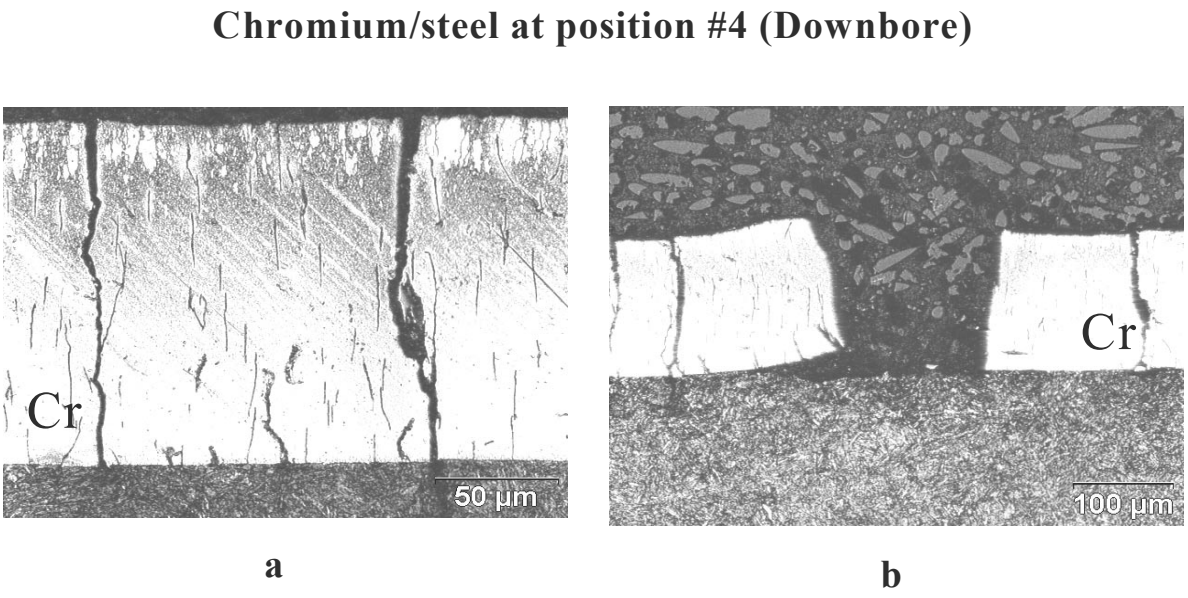

Figure 7. Micrograph showing sections through specimens from position 4 (downbore). There is no heat affected zone in the steel. Chromium cracking, chromium loss and high temperature corrosion are observed.

Note also the cupping of the top surface of the chromium island. This is a commonly observed feature showing significant plastic deformation of the softened chromium as a result of thermal stressing upon cyclic heating. The figure suggests that debris is a contributing factor in enhancing the cupping effect. Figure 7b illustrates that plastic deformations associated with chromium loss can be very large. Such deformations cannot occur at low temperatures because of the brittleness of the chromium.

Figure 8 shows ABAQUS finite element model results on the residual deformation near two cracks after a pre-cracked gun section has been exposed to a severe tank round heat pulse. (ABAQUS is a finite element software package developed by Hibbitt, Karlsson, and Sorensen, Inc.) The planar model (radial-circumferential) included an elastic, perfectly plastic material definition for steel with a yield stress of 170 ksi. Plane strain boundary conditions were assumed with no axial strain. Prior to being exposed to the heat load, the crack face surfaces were assumed to be in intimate contact with each other

(no separation). Symmetry planes on the right and left side of the model section were enforced by permitting only radial movement for nodes on these surfaces. Each crack was assumed to be 0.005 in. deep with a crack spacing of 0.005 in. The scale factor on the deformation in the figure is 20. The model results reproduce the main features of cupping effect seen in Figure 7.

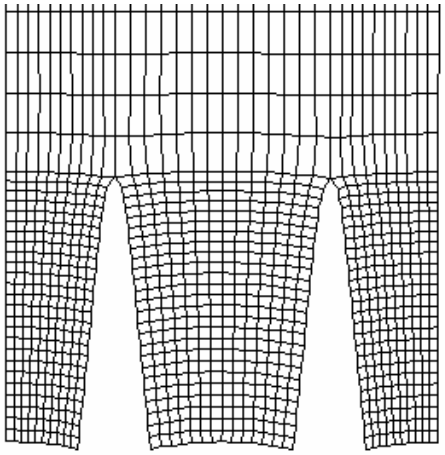

Figure 8. Finite element model results illustrating permanent deformation produced in the chromium islands by high temperature stresses and plastic deformation. Finite element model showing residual deformation (cupping effect) in the vicinity of two cracks after thermal loading.

Figure 9 is an example of similar large plastic deformations found in the chamber at position no. 2. Again, these large plastic deformations must be high-temperature effects because of the high hardness and brittleness of high contractile chromium at low temperatures. The darkening of the chromium islands is caused by enhanced etching associated with recrystallized chromium and reflects the high heating that occurs during firing whenever chromium islands separate from their substrate heat sink. The type of curvature in this figure is often observed in the lifted chromium islands.

Large curvature exhibited by disbonded chromium islands

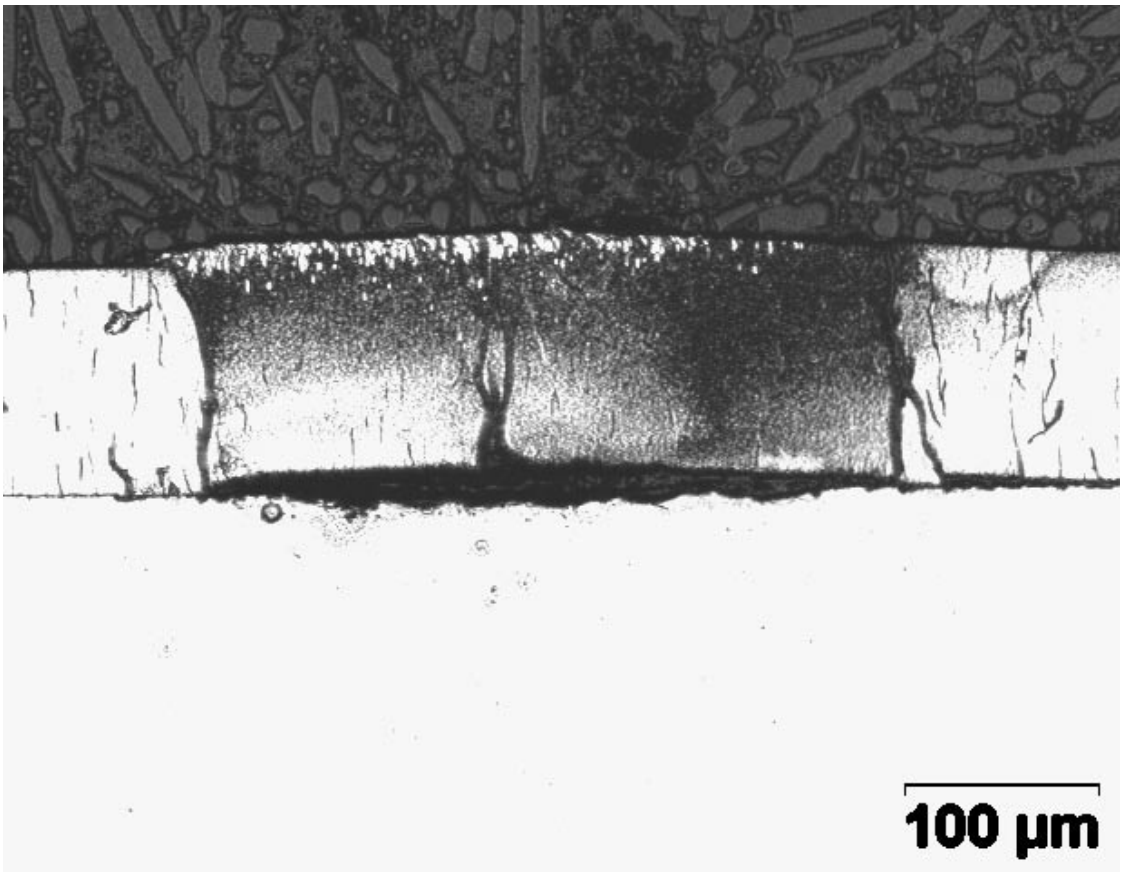

Figure 9. Micrograph showing an example of the general phenomenon of island lifting. Large curvature exhibited by disbonded chromium islands

DISCUSSION

Tube Expansion/Thermal Stress

The preferential lifting of the chromium edges that are oriented along the tube axis indicates that mechanical dilation of the chamber provides a major damage mechanism for the chromium islands at these locations. Thermal strains are expected to be low in the chamber, given the relatively low temperatures expected there. Using the chamber wall ratio of 2 gives chamber strains of approximately

0.6% at 689 MPa (100 ksi). The observed damage cannot occur during the pressurization stage because pressurization produces island separation. Thus, the observed edge lifting probably occurs on depressurization as a result of debris that is forced into the cracks during pressure rise. The reduced amount of edge lifting at position no. 1 may be attributed to its proximity to the bearing surface of the breech ring, which constrains chamber dilation. Similarly, there is little evidence of preferential edge lifting at or near positions no. 3 and no. 4 in the bore, where biaxial thermal strains are expected to dominate over the mechanical strain from pressurization (estimated at ~0.5% for a wall ratio of 2.4 at 689 MPa).

Oxidation

High-temperature oxidation of the steel at the chromium crack tips and along the interface is evidently an essential factor for chromium loss, as oxidation generally accompanies chromium edge lifting and chromium island separation. The growth and linkage of embedded cracks within the chromium islands (in high contractile chromium) allow gas penetration to the interface, which promotes steel oxidation all along the interface of the individual chromium islands. Once the chromium islands are lifted from the substrate, rapid steel consumption can then generate deep pits in the steel. The pitting process in the form of high temperature oxidation actually begins before chromium islands are lifted away. Often there is considerable oxidation beneath the chromium. It should noted that sulfur is another very aggressive corrosion agent that can produce high temperature corrosion damage similar to oxidation (ref 1)**.** The absence of chromium loss at position no. 1 (midchamber) and the observation that very little corrosion is observed at the interface at this location is consistent with the view that high temperature corrosion is the primary cause of chromium spallation.

While aqueous corrosion from moisture in the gun tube cannot be ruled out completely as a contributing factor to pitting in the chamber, it does not appear to be significant. The main reason is that firing debris usually fills chromium cracks and pits with a protective glaze that seems to be effective in suppressing the rusting process. Inspection of steel in the numerous pitted areas generally shows only evidence of high temperature damage such as heat affected zones, oxide scale, and carburization.

Chromium Softening and Substrate Softening

The observation that chamber heating is insufficient to cause chromium softening there (Table 1) may actually be a reason for enhanced chromium loss in the chamber. Soft chromium will be more resistant to spallation because chromium yielding can reduce stress transfer to the interface. Permanent chromium softening from heating during firing is observed in the bore. Maximum softening occurs at the bore origin (position no. 3), which is probably one of the reasons for the absence of any chromium loss at that location.

The numerous chromium cracks shown in the micrographs for position no. 2 reflect the brittle nature of the chromium in the chamber. This contrasts with the micrographs for bore positions no. 3 and 4, where there is clear evidence of extensive plastic flow in the softened chromium.

A benefit of substrate heating on firing is, again, a yield strength reduction (softening) that accompanies the temperature rise of the steel adjacent to the chromium. As in the coating, softening of the substrate adjacent to the interface will also permit plastic flow to act as a buffer against firing stresses that cause the chromium islands to spall. As discussed in Cote et al. (ref 2), formation of a heat-affected zone implies a transformation to the soft austenite phase, which is retained during most of the firing cycle and, thus, should be a buffer against firing stress damage to the interface. This effect is likely to be another reason for the chromium retention at the bore origin (position no. 3).

Embedded Cracks

One of the more remarkable features associated with damage in high contractile chromium is the permeation of corroding propellant gas throughout the network of embedded cracks that exist in each of the chromium islands. Although much of the fracture and corrosion damage to the steel substrate occurs at the tips of the major chromium cracks that serve to define the individual islands, the general permeation of corroding gas through the embedded cracks to the interface must further exacerbate chromium spallation. For this reason, sputtered chromium or low contractile electro-deposited chromium should offer more resistance to chromium loss than high contractile chromium because embedded cracks do not occur in these coatings. As with high contractile chromium, however, a large

number of major cracks are expected to develop during firing with sputtered chromium or low contractile chromium coatings.

Chromium Diffusion

Chromium diffuses readily into steel at elevated temperatures. As a result, the original interface is replaced by an interdiffusion zone, consisting of a chromium enriched steel layer. This effect is similar to the commercial "chromizing" process, which is used to protect steel against high temperature oxidation. We have observed interface shifts associated with preferential diffusion of chromium into steel (Kirkendall effect) in chromium-plated specimens from fired components, laser pulse heated specimens, and in vented combustor specimens whenever there is a heat-affected zone generated in the steel substrate. In these cases, the diffusion is manifested by a distinct alloy layer at the interface, visible when the specimen is etched for both chromium and steel. It has the beneficial effect of protecting the vulnerable interface zone from rapid, high-temperature oxidation. Chromium diffusion is observed at position no. 3 (bore origin), as expected, because there is a heat-affected zone in the steel at this location. Thus, chromium diffusion is another factor (along with chromium softening and heat affected zone softening) that resists chromium coating spallation at locations that have experienced high heating (e.g., position no. 3). Without the protection offered by the "chromized" interface, oxidation will rapidly progress along the interface, in analogy with enhanced diffusion along grain boundaries.

Gas Trapping/Firing Debris

The simplest explanation for the general phenomenon of island lifting is gas pressurization beneath the chromium islands. Given the general observation of firing debris deposited in the chromium cracks, and the development of erosion pockets beneath the chromium, one can expect transient gas entrapment in the pockets beneath the chromium islands during rapid pressurization and depressurization.

Surface grinding

Gawne (ref 3) has shown that electro-deposited chromium is susceptible to sliding fatigue in pin-on-disk experiments. The failure mode is fatigue cracking with chromium cracks running parallel to the

surface. Thus, the chromium damage shown in Figures 4d and 6c is consistent with sliding fatigue. Because the grinding operation, at thousands of rpm, produces substantial material removal, it is more severe than pin-on-disk tests, so one must consider that grinding severely damages the chromium in the chamber. The required amount of grinding will vary from one tube to another, so this process could account for tube-to-tube variations in pitting development.

Adhesion

Achieving optimum adhesion is usually a challenge, and, because of process variations, chromium adhesion can vary from tube-to-tube. As discussed above, it is likely that the high chromium hardness places particularly high demands on chromium adhesion in the chamber area. Thus, it is possible that some of the reported randomness in pitting severity from tube-to-tube is related to adhesion variations.

Mixed Mode Fracture at the Interface

We assumed throughout that thermal and mechanical forces acting on the chromium islands are transmitted to the interface to produce spallation of the chromium from the steel, and that this spallation is aided by hot corrosion along the interface. The essential mechanics can be understood in terms of a mixed mode fracture at the chromium island edges using finite element modeling. (Underwood et al. [ref 4] address the problem in terms of a model where shear strength failures at the coating interface originate from high thermal gradients). The present results are discussed in terms of forces acting on the chromium island that propagate both peeling (mode I) and shear (mode II) fracture at the corrosion-degraded interface. Corrosion assisted fatigue is the most likely mechanism that produces spallation of the coating, in view of the evidence for progressive failure at the interface. The model is that of an isolated chromium island on a constrained steel substrate as illustrated in Figure 10. The steel is constrained against any lateral dilation from the thermal load by the large bulk of the surrounding cold steel in the walls of the chamber and bore. The crack spacing is typically twice the coating thickness (~100 μm) with high contractile chromium, so we assume a disk radius of 100 μm.

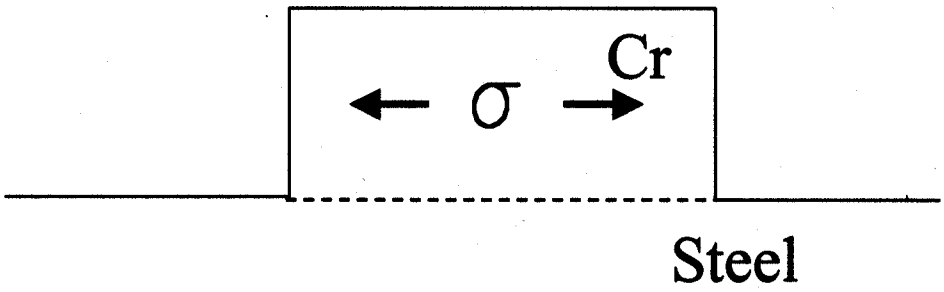

Figure 10. Schematic of an isolated disc shaped chromium island on a steel substrate.

FEMLAB was used to perform finite element modeling of the configuration shown in Figure 10. (FEMLAB is a software package developed by COMSOL Inc.) The model generates interface stresses from the thermal and mechanical loading of the coating during firing. The thermal loading is accomplished by uniformly heating or cooling the axisymmetric structure (disk) shown in Figure 11 with applied substrate constraints, as shown, to represent the constraint of the steel substrate applied by the cold outer wall of the gun tube. (Thermal gradients are present, but our model results have shown that assuming an average peak coating temperature of 1000ºC is sufficient to illustrate the nature and approximate magnitude of stresses that are expected during firing.)

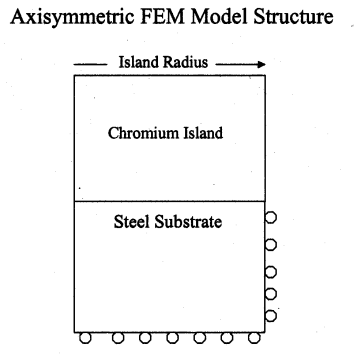

Figure 11. Finite element axisymmetric model structure of a chromium island on a constrained steel substrate.

The shear stresses and peeling stresses resulting from cooling through a temperature range of 1000C are shown in Figure 12. It is assumed that during the cooling phase, the system stress starts from essentially zero at high temperatures because of high temperature yielding. The stresses can increase on cooling because the low temperature yield strength is high.

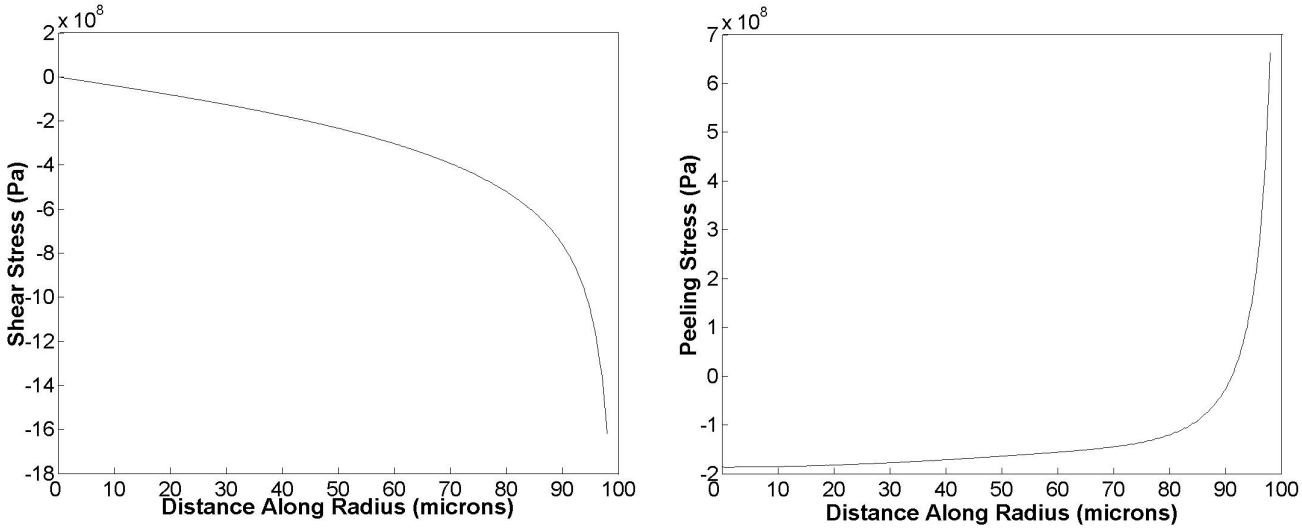

Figure 12. Finite element model results showing distribution of shear stress and peeling stress for a chromium island attached to a constrained steel substrate and cooled through a temperature range of 1000ºC.

The stress characteristics illustrated in Figure 12 are universal in the sense that for most types of loads applied to a chromium island on a constrained substrate, shear and peeling stresses will occur at the interface and will increase rapidly in magnitude near the edge. The stresses rise beyond the gigapascal range within 5–10 μmof the island edge on both heating or cooling through the 1000ºC temperature range; however, there is a reversal in sign of both the shear stresses and peeling stresses for the heating and cooling cases. The magnitudes of the shear and peeling stresses are well in excess of the yield and tensile strength of the material near the coating edge, indicating that significant yielding must occur at that location with every firing for the coating to survive (see Figures 7 and 8). The stresses rise rapidly at the island edge because of the sharp corner and substrate constraint. When cracks and corrosion propagate into the substrate, a reduction in the magnitude of both shear and peeling stresses will occur because the “singularity” associated with a sharp corner and constraint is removed or

displaced into the substrate. Thus, there can actually be advantages in terms of a reduction in spallation forces when cracks and corrosion extend directly into the steel substrate. On the other hand, corrosion that propagates along the interface is, of course, detrimental because it will tend to maintain high shear and peeling stresses at the interface.

Similar model results are found when one applies mechanical stress to the substrate to simulate the effect of hoop stresses during firing. Assuming firing pressures of 690 MPa (100 ksi) gives shear stress magnitudes roughly one-half those shown in Figure 12 from thermal stress. The effect of uniform pressurization along the chromium side walls was also modeled: the same features are exhibited as with the thermal and hoop stress loading, but the magnitudes of the stresses are approximately one tenth of the model results with thermal loading, indicating that this effect can usually be neglected.

For the case of the predominant mechanical loading on pressurization in the chamber, the coating stress, σ, can be considered the algebraic sum of stresses exerted by the tensile hoop stress, the gas pressure, and any thermal stress. On depressurization, as discussed above, the micrographs indicate that there is a significant contribution to σ arising from interference from trapped firing debris (preferential edge lifting) during hoop stress relaxation of the chamber wall. In the bore areas, the maximum surface temperatures during firing were clearly higher than in the chamber, so thermal stresses are expected to dominate in the bore.

Regarding the role of compressive thermal stresses that arise in the coating during heating, there are a number of reasons why the stresses caused by heating may be less effective than those from cooling in promoting spallation. First, the interface stress is likely to be reduced because of contact with adjacent chromium islands and with the firing debris wedged in the chromium cracks. Second, yield strength reductions and metal flow at high temperatures will limit the tendency for interface fracture because ductility tends to blunt cracks. And third, the peeling stresses at the island edges are compressive, rather than tensile, which tend to suppress edge fracture. Consequently, it is expected that the stresses developed in the coating on cooling will be the main contributor to chromium spallation.

Note that it is the average peak stress in the coating that drives the mixed mode (peeling and shear) failure at the coating edges (e.g., Figure 4c), so for thermal stresses, the stress magnitude is

determined by average peak coating temperature. Thus, one might expect that the chromium islands at position no. 3 experience higher spallation forces than at other positions. No chromium loss is observed at position no. 3, however. As discussed above, the substantial permanent chromium softening, the plastic flow in the austenitic substrate during cooling, the reduction in the sharp corner "singularity" accompanying the relatively deep cracks and corrosion at the chromium crack tips at that location, and the protective "chromizing" process, all can serve to suppress the thermochemical and thermomechanical damage expected at position no. 3 (bore origin).

SUMMARY

A representative M256 tank gun tube was selected for analysis of chromium loss mechanisms along the critical regions of the 120-mm gun chamber and bore. A common feature at all chromium loss locations is significant high temperature corrosion (oxidation in this case) at the interface. High temperature corrosion serves to undermine the chromium and facilitate chromium spallation. The exposed steel can then be rapidly consumed by the corrosion process to produce pitting in the chamber and melt/erosion in the bore. In the chamber area, pitting can be severe enough to affect the service fatigue life. The data indicate the presence of a wide variety of additional contributing factors, so that the specific factors responsible for chromium loss are likely to differ from one location to another.

REFERENCES

1. Cote, P.J. and Rickard, C., "Gas-Metal Reaction Products in the Erosion of Chromium Plated Gun Bores," *Wear*, vol. 241, 2000, pp 17–25; Tech. Report ARCCB-TR-99016.

2. Cote, P.J., Lee, S.L., Todaro, M.E., and Kendall, G., "Application of Laser Pulse Heating to Simulate Thermomechanical Damage at Gun Bore Surfaces," Tech Report ARCCB-TR-03002.

3. Gawne, D.T., "Failure of Electrodeposited Chromium Coatings on Cast Iron Substrates," *Thin Solid Films*, vol. 118, 1993, pp 385–393.

4. Underwood, J.H., Witherell, M.D., Sopok, S., McNeil, R., Mulligan, C., Vigilante, G., "Thermomechanical Modeling of Transient Thermal Damage in Cannon Bore Materials," *Proceedings of 16 US Army Symposium on Solid Mechanics, Charleston, SC*, 4–7 May 2003.